Case Report

Liquid biopsy perspectives in pleomorphic carcinoma of the lung: case report

Tania Rossi[1#], Michela Cortesi[1#], Michele Zanoni[1#], Sara Bandini[1], Camilla Sbrighi[1,2], Davide Angeli[3], Valentina Masciale[4], Giulia Grisendi[4], Matteo Costantini[5], Franco Stella[6], Paola Ulivi[1*], Beatrice Aramini[6*^]

[1]Biosciences Laboratory, IRCCS Istituto Romagnolo per lo Studio dei Tumori (IRST) "Dino Amadori", Meldola, Italy; [2]Department of Biomedical and NeuroMotor Sciences, University of Bologna, Bologna, Italy; [3]Unit of Biostatistics and Clinical Trials, IRCCS Istituto Romagnolo per lo Studio dei Tumori (IRST) "Dino Amadori", Meldola, Italy; [4]Laboratory of Cell Therapies, Department of Medical and Surgical Sciences for Children & Adults, University Hospital of Modena, Modena, Italy; [5]Unit of Pathology, G.B. Morgagni-L. Pierantoni Hospital, Forlì, Italy; [6]Division of Thoracic Surgery, Department of Medical and Surgical Sciences-DIMEC, Alma Mater Studiorum, University of Bologna, G.B. Morgagni-L. Pierantoni Hospital, Forlì, Italy

Contributions: (I) Conception and design: B Aramini, T Rossi; (II) Administrative support: B Aramini, T Rossi, P Ulivi; (III) Provision of study materials or patients: B Aramini, F Stella, M Costantini; (IV) Collection and assembly of data: B Aramini, T Rossi, M Costantini, M Zanoni, S Bandini, C Sbrighi, D Angeli, V Masciale, G Grisendi, F Stella, P Ulivi; (V) Data analysis and interpretation: B Aramini, T Rossi, M Costantini, M Zanoni, D Angeli, P Ulivi; (VI) Manuscript writing: All authors; (VII) Final approval of manuscript: All authors.

[#]These authors contributed equally to this work as co-first authors.

[*]These authors contributed equally to this work as co-last authors.

Correspondence to: Beatrice Aramini, MD, PhD. Division of Thoracic Surgery, Department of Medical and Surgical Sciences-DIMEC, Alma Mater Studiorum, University of Bologna, G.B. Morgagni-L. Pierantoni Hospital, Campus of Forlì, Via Carlo Forlanini n. 34, 47121 Forlì, Italy. Email: beatrice.aramini2@unibo.it.

Background: Liquid biopsy has recently made it possible to use minimally invasive testing to examine tumor-derived material released into peripheral blood, including circulating tumor cells (CTCs), extracellular vesicles (EVs), and circulating tumor deoxyribonucleic acid (ctDNA). Lung pleomorphic carcinoma (PC) is an extremely rare and severe form of cancer. Although resection tissues are the basis for PC diagnosis in everyday practice, tiny biopsies and cytologic specimens might potentially raise suspicions. Because PC may show varied expression of conventional carcinoma markers, it can be particularly challenging to differentiate sarcomatoid (i.e., spindle cell or giant cell) components from other tumor forms, such as sarcomatoid mesothelioma and other sarcomas. We think that defining a more specific context to better understand patient prognosis may be aided by the discovery of blood molecular markers in PC.

Cases Description: We present two cases of patients underwent major lung resection at our center with a diagnosis of PC of the lung; specifically, according with 8th TNM edition, case 1 showed a final pathological stage pathological tumor-node-metastasis (pTNM): pT1cN0G3LV0R0, and case 2 showed a stage pTNM: pT3N0G3LV0R0. Patients were both discharged after surgery with no postoperative complications. Oncologists suggested a 5-year clinical and radiological follow-up, however case 1 patient is free from recurrence at the moment, while case 2 patient died for brain recurrence 10 months after surgery. Immediately after surgical resection, patient's specimens were sent to the pathology unit. The pathologist, without affecting the accuracy of histological diagnosis, selected representative tissue samples and sent them at 4 ℃ in specific media, to Bioscience Laboratory, IRCCS IRST "Dino Amadori" for tissue analysis. Additionally, blood samples collected before surgery were sent for the characterization of CTCs and EVs.

Conclusions: To better characterize the potential relationship between the presence of CTCs, EVs and high grade of malignancy and any subsequent connection to death and/or recurrence, we think that liquid biopsy, which involves the identification and characterization of tumor-derived elements, may serve as future

^ ORCID: 0000-0002-5326-710X.

© AME Publishing Company.

approach and tool not only in NSCLC but also in each specific histotype as for lung PC.

Keywords: Circulating tumor cells (CTCs); extracellular vesicles (EVs); liquid biopsy; lung cancer; case report

Submitted Dec 29, 2024. Accepted for publication Apr 03, 2025. Published online Jun 19, 2025.
doi: 10.21037/tlcr-2024-1275
View this article at: https://dx.doi.org/10.21037/tlcr-2024-1275

Introduction

More people die from lung cancer in the US than from any other kind of cancer combined (1). The last 15 years have seen a significant evolution in the treatment of lung cancer, especially non-small cell lung cancer (NSCLC). The treatment of NSCLC has emerged as a notable instance of precision medicine in the context of solid tumor cancers (2).

Blood-based diagnostics may be able to noninvasively provide comparable, clinically valuable information in certain situations, even though tissue biopsies are still important and serve a variety of functions in the treatment of NSCLC (3).

Molecular profiling, clinical staging, and pathologic findings are now key components of NSCLC clinical management (2-4). The preferred treatment option for metastatic NSCLC patients carrying a targetable alteration is targeted therapy. This type of treatment has also been recently approved in the neo-adjuvant (NeoADAURA) and adjuvant settings (ADAURA) (5).

The conventional method for molecular profiling is based on the analysis of tumor tissue. Recently, liquid biopsy has enabled the investigation of tumor-derived material shed into peripheral blood, such as circulating tumor cells (CTCs), extracellular vesicles (EVs), and circulating tumor deoxyribonucleic acid (ctDNA), through minimally invasive testing (6,7). Specifically, numerous studies have assessed the prognostic significance of CTCs in lung cancer, however the results are debatable (6-8). Furthermore, there is insufficient data to determine the function and prognostic significance of CTC measurements in the various histological subtypes of lung cancer as well as at various stages of the disease, including before and after treatment. Even less is known about the function of various CTC subpopulations, such as epithelial or mesenchymal CTCs (6-9).

Over the past few decades, a number of findings regarding the pathophysiology of lung cancer have resulted in the creation of novel targeted treatments and the recognition of the pivotal function of the host immune system and response (10-12). Furthermore, there is growing evidence that EVs participate in the growth and development of tumors, indicating their potential utility as prognostic and diagnostic biomarkers for lung cancer. However, methodological heterogeneity should be critically examined before utilizing these particles in routine clinical practice as it may result in unclear outcomes. In this paper, we describe EVs and CTCs that were extracted from the bloodstream of two patients with pleomorphic carcinoma (PC) before surgery. Copy number aberration (CNA) profiling showed varying degrees of heterogeneity in the patients' clusters of white blood cells and CTCs. Moreover, EVs analysis revealed the expression of markers linked to platelets. In order to better understand this uncommon tumor type, we present, for the first time, to the best of our knowledge, probably for the rarity of this tumor

Highlight box

Key findings

- In this manuscript, we characterize circulating tumor cells (CTCs) and extracellular vesicles (EVs) isolated from the bloodstream of 2 patients with pleomorphic carcinoma before surgery. The patients presented clusters composed of CTCs and white blood cells, and copy number aberration profiling revealed degrees of heterogeneity. EV analysis showed the expression of platelet-associated markers.

What is known and what is new?

- The investigation of CTCs and EVs provides valuable insights across various cancer types, including lung tumors, through a liquid biopsy approach.
- To the best of our knowledge, we report for the first time a detailed characterization of tumor-derived elements retrievable in the bloodstream of patients with pleomorphic cancer, contributing to the understanding of this rare tumor type.

What is the implication, and what should change now?

- Further studies involving CTCs and EVs are necessary to gain a more comprehensive understanding of the biology of pleomorphic lung cancer.

© AME Publishing Company.

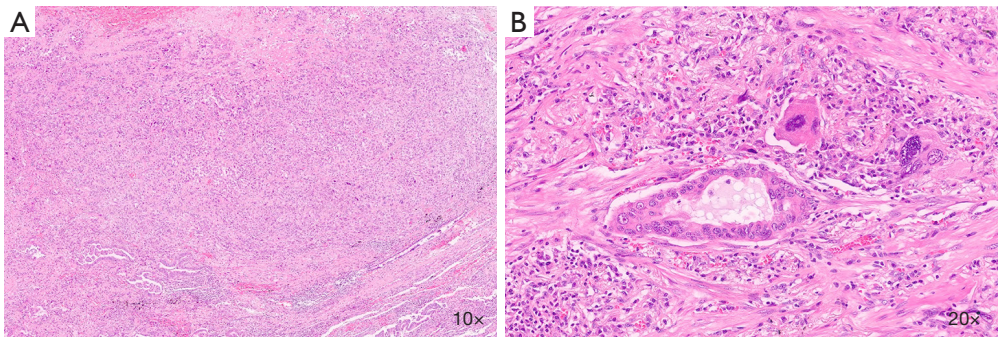

Figure 1 Microscopic hematoxylin and eosin photograph of tumor tissue from case 1. (A) Histological image colored in hematoxylin-eosin, 10× magnification, presence of an adenocarcinoma component and a poorly differentiated spindle cell and pleomorphic component. (B) Histological image colored in hematoxylin-eosin, 20× magnification, detail of a neoplastic glandular structure and some pleomorphic cells.

among lung cancers, a thorough characterization of tumor-derived elements that can be recovered in the bloodstream of patients with pleomorphic cancer. However, additional research utilizing CTCs and EVs is required to comprehend the biology of pleomorphic lung cancer more thoroughly.

PC of the lung is a very uncommon and aggressive type of cancer. PC diagnosis in daily practice is based on resection specimens, but it can also be suspected based on small biopsies and cytologic specimens.

It can be especially difficult to distinguish sarcomatoid (i.e., spindle cell or giant cell) components from other tumor types, such as sarcomatoid mesothelioma and some sarcomas, because PC may exhibit variable expression of typical carcinoma markers (13,14).

We believe that the identification of blood molecular markers in PC may be helpful to define a more detailed setting to better understand patient prognosis. We present this article in accordance with the CARE reporting checklist (available at https://tlcr.amegroups.com/article/view/10.21037/tlcr-2024-1275/rc).

Cases presentation

Case 1

A 72-year-old man came to our center in 2022 for an accidental finding of a lung nodule in the left upper lobe. He declared to be a heavy smoker (80 packs/year) with a medical history of diabetes and hypertension. He referred a persistent cough with haemoptysis episodes, for one month for whom he underwent an otolaryngologist examination, who found blood in the upper respiratory tract, suggesting to perform a more accurate radiological check. A chest computed tomography (CT) scan with contrast enhancement highlighted the presence of a pulmonary nodule measuring 2.7 cm × 1.8 cm at the left upper lobe.

A ^{18}F-fludeoxyglucose total body positron emission tomography/computed tomography (^{18}F-FDG TB PET/CT) scanning showed hypermetabolism at the level of the nodule (SUVmax =10.62). A transbronchial needle aspiration of the nodule was positive for malignant lesion, as NSCLC, to further characterize. Pulmonary respiratory function was normal forced expiratory volume in 1 second (FEV_1) 3.40 (106%), forced vital capacity (FVC) 4.26 (103%), diffusing capacity of the lung for carbon monoxide (DLCO) 7.66 (83%), alveolar volume (VA) 6.68 (97%).

In consideration of the diagnosis, he underwent left upper lobectomy at our center by videothoracoscopic approach (VATS) with a histopathological diagnosis of poorly differentiated NSCLC (G3), pleomorphic. The neoplasm consisted partly of an infiltrating acinar adenocarcinoma with a central portion greater than 10% of the neoplasm, large cells with abundant eosinophilic cytoplasm and pleomorphic nuclei, and with spindle cell foci. The two components expressed cytokeratin 7 and cytokeratin adverse event (AE) 1–3 differently, the amount of adenocarcinoma with intense diffuse positivity, the pleomorphic portion with weak, focal positivity. The neoplastic tumors in both components expressed thyroid transcription factor 1 (TTF1) in a variable manner; negative p40. No evidence of lymphovascular and/or pleural invasion (*Figure 1A,1B*). Final pathological stage (pTNM): pT1cN0G3LV0R0 (8th edition TNM).

The patient was discharged from surgery in four days without complications. For the final diagnosis, the

© AME Publishing Company.

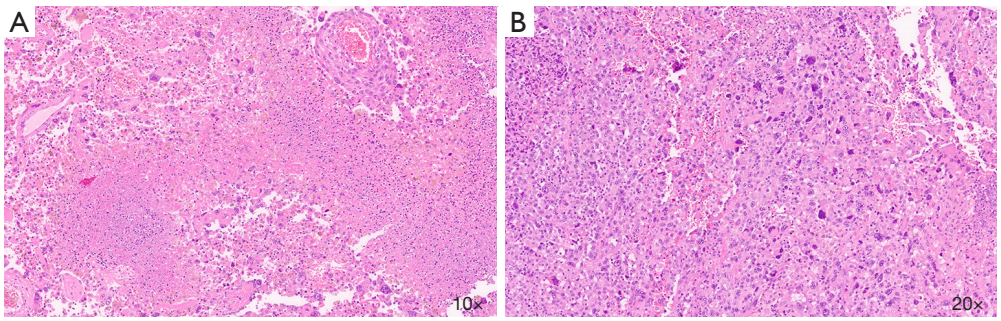

Figure 2 Microscopic hematoxylin and eosin photograph of tumor tissue from case 2. (A) Histological image stained in hematoxylin-eosin 10× magnification: squamous carcinoma component and poorly differentiated component with pleomorphic cells. (B) Histological image stained in hematoxylin-eosin, 20× magnification: detail of the pleomorphic cell component.

oncologist suggested clinical and radiological follow-up for 5 years from surgery. At the moment patient is free from recurrence.

Case 2

A 75-year-old man came to our attention in June 2022, sent by his doctor for the diagnosis of a left lung opacity after chest X-ray performed for recurrent cough and dyspnea occurring for two months since March. As for past medical history, he referred heavy smoking history (120 packs/year), a meningioma under radiological follow-up, chronic obstructive pulmonary disease (COPD), hypertension, and diabetes. He then performed a chest CT with contrast enhancement, confirming the neoformation in the apical segment of the left lower lobe of the lung. A ^{18}F-FDG TB PET/CT scanning highlighted a hypermetabolism at the level of the lesion with SUVmax equal to 15.18. A needle CT biopsy has been performed with a diagnosis of malignant tumor of the lung, inclined towards adenocarcinoma. Pulmonary respiratory function showed a moderated obstructive condition with FVC 2.15 (63%), FEV_1 1.41 (55%), DLCO 4.93 (64%), VA 5.21 (84%).

After the anesthesiologist's consent, patients underwent left lower lobectomy by VATS with no postoperative consequences. He was discharged from hospital after five days. The final histopathological diagnosis showed a pleomorphic, infiltrating and poorly differentiated NSCLC (G3) with no evidence of infiltrating lymph nodes. Carcinoma cells showed variable positivity for cytokeratin AE 1–3 and cytokeratin 7; weak and focal positivity for TTF1 (*Figure 2A,2B*). Final pathological stage (pTNM): pT3N0G3LV0R0. The patient was discharged after five days from surgery with no postoperative complications.

For the stage, the oncologists suggest a 5-year clinical and radiological follow-up, however patient died from brain recurrence 10 months after surgery.

The patients involved in the study were recruited by the Thoracic Surgery Unit of the Morgagni Pierantoni Hospital in Forlì, FC, Italy. All the experiments were undertaken with the understanding and written consent of each subject. All procedures performed in this study were in accordance with the Declaration of Helsinki and its subsequent amendments, and local laws and fulfilled Regulation (EU) 2016/679 of the European Parliament and the Council of April 27, 2016, on the protection of natural persons regarding the processing of personal data. The present study has been approved by the local ethics committee (Comitato Etico di IRST e di Area Vasta Romagna, CEROM IRSTB129).

Tumor tissue dissociation and immunophenotypic analysis

Immediately after surgical resection, performed as per clinical practice, the patient's specimens were sent to the pathology unit. The pathologist, without affecting the accuracy of histological diagnosis, selected representative tissue samples and sent them at 4 °C in specific media to Bioscience Laboratory, IRCCS IRST "Dino Amadori". To dissociate cancer tissue, the Tumor Dissociation Kit, human (Miltenyi) was used according to the manufacturer's protocol. In brief, surgically resected lung tumor tissues were mechanically dissociated and transferred into genteMACS C Tube for enzymatic dissociation for 1 hour at 37 ℃. Dissociated cells were then filtered using a MACS SmartStrainer (70 µm). Cells from digested tumor tissues were subjected to immunophenotypic analysis. Briefly,

© AME Publishing Company.

1×10^6 cells were incubated with FcR Blocking Reagent human (Miltenyi Biotec) at 4 ℃ for 10 minutes, to limit the non-specific binding of the antibodies used. Then, cells were incubated with anti-CD44 (Miltenyi; 1:100), anti-CD326 (Miltenyi; 1:100) and anti-CD45 (Miltenyi; 1:100) at 4 ℃ for 30 minutes. Cells were finally washed in 1X PBS and read at Attune NxT® cytometer (Thermo Fisher). The values in % of CD44+, CD326+ and CD44+/CD326+ were obtained by subtracting the % positivity of the negative control from the % positivity of each marker.

CTC isolation and CNA analysis

To investigate CTCs in patients with lung cancer, approximately 18 mL of peripheral blood was collected in EDTA tubes before surgery. CTC enrichment was conducted by adding RosetteSep CTC Enrichment Cocktail containing anti-CD36 (StemCell) to whole blood (50 µL reagent/mL blood), and gradient centrifugation was performed using Sep-Mate Tubes (StemCell) following the instructions provided by the manufacturer. Finally, CTCs were vitally cryopreserved in a freezing solution containing fetal bovine serum (FBS) +10% dimethyl sulfoxide (DMSO) until phenotypic analysis. To detect CTCs, cellular pellets derived from enriched fractions thawed by gently pipetting RPMI 1640 culture medium (GIBCO, Invitrogen, Ireland) +10% FBS at 37 ℃ and subjected to antibody staining using a cocktail of antibodies targeting epithelial markers (E-tag) CD326 (clone HEA-125; 1:10 dilution; phycoerythrin, PE channel) and E-cadherin (clone 67A4; 1:10 dilution; phycoerythrin, PE channel), while anti-CD45 (clone HI30; 1:10 dilution; fluorescein-5-isothiocyanate, FITC channel) was used for leukocyte visualization. Hoechst33342 (1 µg/mL; ThermoFisher Sc.) was used in the 4′-6-diamidino-2-phenylindole (DAPI) channel for nuclear staining. CTC detection and recovery were performed using the DEPArray NxT platform (Menarini Silicon Biosystems).

Cells were isolated as single, viable cells, then subjected to whole genome amplification (WGA) to obtain evaluable deoxyribonucleic acid (DNA) using the Ampli1™ WGA kit (Menarini Silicon Biosystems). The quality of each WGA product was checked using the Ampli1 QC kit by amplifying 4 conserved regions of the genome by polymerase chain reaction (PCR). The final product was visualized using Chemidoc XRS; the DNA of each sample was considered suitable for downstream analyses when the number of amplified regions was ≥2.

For CNA analysis, libraries were prepared using the Ampli1™ Lowpass kit for Ion Torrent (Menarini Silicon Biosystems). The Ion chips were prepared using the Ion Chef and sequenced using the Ion Torrent S5 sequencing system (Thermo Fisher Scientific). Bioinformatic analyses were conducted as reported in our previous publications (15-17).

Analysis of EVs

EVs were isolated starting from 1 mL of plasma using the qEV10 size exclusion columns (70 nm, Izon Science) following the instructions provided by the manufacturer. The EV-enriched fractions were collected.

The concentration (number/mL) and particle size (nm) of EVs were obtained through nanoparticles tracking analysis (NTA) using the NanoSight NS300 (Malvern Panalytical) equipped with NTA 2.3 analytical software laser. All samples were diluted 1:100 in filtered D-PBS 1X, and subsequently, three videos of 30 s each per sample were recorded at a camera level of 15 and in light scattering mode following the guidelines of the manufacturer.

EV's surface proteins were characterized through a bead-based multiplex analysis by flow cytometry (MACSPlex Exosome kit, human; MiltenyiBiotec, Bergisch Gladbach, Germany). This method allows for the analysis of 37 different epitopes on the surface of the EVs including specific markers for the identification of exosomes (CD9, CD81, CD63). Briefly, 10 µg of protein for each sample was diluted in MACSPlex buffer to obtain a final volume of 120 µL. Then, each diluted sample was incubated for 1 hour at room temperature on an orbital shaker at 450 rpm with different antibody-coated bead subsets and APC-conjugated anti-CD9, anti-CD63, and anti-CD81 detection antibodies. The samples were analyzed with the Attune Nxt flow cytometer (Thermo Fisher Scientific), obtaining the raw value of the median fluorescence intensity (MFI) for each epitope. The MFI value of the negative control was subtracted from the obtained raw MFI value of each epitope, then the data were normalized on the MFI of the tetraspanins CD9, CD63, and CD81.

Immunophenotypic evaluation of pleomorphic lung cancer tissues

Firstly, to perform a characterization of the primary pleomorphic lung tumors, we evaluated the presence of epithelial and stem cell populations using a cytometric-based method and compared them to data obtained from lung tumor samples of other lung cancer histotypes. More

© AME Publishing Company.

Table 1 Results of immunophenotypic investigation and percentage of different phenotypic cell populations in different lung tumor tissues

Patient ID (code)	Histology (histotype)	EPCAM+ (%)	CD44+ (%)	EpCAM+, CD44+ (%)
Case 1	NSCLC, pleomorphic	18.56	3.33	0.38
Case 2	NSCLC, pleomorphic	1.44	0.08	0
Squamous 1	Squamous carcinoma	28.9	10.83	10.23
Squamous 2	Squamous carcinoma	26.2	17.2	2.53
Neuroendocrine 1	Neuroendocrine	84.7	0.11	0.7
Neuroendocrine 2	Neuroendocrine	80.7	0.25	16.69
Adenocarcinoma 1	Adenocarcinoma	71.16	7.74	5.76
Adenocarcinoma 2	Adenocarcinoma	69.41	2.68	2.27
Adenocarcinoma 3	Adenocarcinoma	79.7	1.94	1.83

ID, identity document; NSCLC, non-small cell lung cancer.

specifically, we considered as control samples, patients with a diagnosis of adenocarcinoma (n=3), squamous-cell carcinoma (n=2) and neuroendocrine tumors (n=2), that were matched for sex and age (mean age =73.57 years; min =67 years; max =77 years). For each sample, we assessed the percentage of epithelial [epithelial cell adhesion molecule (EpCAM)], stem (CD44+) and dual-positive (EpCAM+/CD44+) cell populations (18).

We obtained 2.9×10^6 cells (vitality =49%) and 28×10^6 cells (vitality =52%) after dissociation of lung tumor tissues obtained from patients case 1 and case 2, respectively. Immunophenotypic analysis of revealed that pleomorphic tumor tissues of patients case 1 and case 2 were highly heterogeneous. In particular, the case 2 specimen had very low levels of epithelial cells (1.44%) compared to 18.56% observed in case 1, while the stem population had a percentage of 0.08% in case 2 compared to 3.33% in case 1. Dual positive cells were not detected in case 2, and in case 1 specimens were very low as well (0.38%) (*Table 1*).

Next, we compared the percentages observed in pleomorphic tissues to those obtained in specimens with other lung cancer subtypes. Although the limited number of cases analysed, we observed that the epithelial cell population was present at low values in pleomorphic tissues (median 10%) compared to squamous (median 27.55%), neuroendocrine (median 82.7%) and adenocarcinoma (median 71.16%) specimens. Concerning stem cell population, the median percentage in pleomorphic tissue was 1.71%, compared to the values observed in squamous (14.02%), neuroendocrine (0.18%) and adenocarcinoma (2.68%) specimens. Lastly, pleomorphic tissue specimens had the lowest median value of dual-positive cells (0.19%), compared to squamous (6.38%), neuroendocrine (8.7%) and adenocarcinoma (2.27%) tumors.

Investigation of plasma-derived EVs

The expression of each surface marker was expressed as MFI. The MFI values of each investigated marker expressed by plasma-derived EVs of PC patients were compared to the values obtained from samples of patients with lung cancer of different histologies, as reported above (*Figure 3*).

Using NTA, we assessed EV concentration and size. Regarding PC patients, we observed a concentration of 1.37e+10 particles/mL with a mean size of 116.9 nm for case 1 (*Figure 3A*), and 6.69e+11 particles/mL with a mean size of 145 nm for case 2 (*Figure 3B*).

Expression of typical EV markers (CD9, CD63, CD81) was observed in all the patients (*Figure 3C,3D*).

Focusing on patients with PC, we observed that CD42a (normalized MFI =642.83) and CD41b (normalized MFI =512.09) were the most expressed marker in patient case 1. In EVs obtained from the plasma of patient case 2, the most expressed markers were CD9 (normalized MFI =128.58) and CD81 (normalized MFI =111.94), followed by CD41b (normalized MFI =110.7). Due to the limited number of cases evaluated in this report, we did not perform a statistical comparison. However, we compared the MFI values of case 1 and case 2 to the median MFI of each group. We observed that some markers were expressed in all the groups (CD8, CD24, CD31, CD41b, CD40, CD42a); CD3 was absent in EVs from pleomorphic tumors, while found expressed in squamous (median MFI =23.79), neuroendocrine (median MFI =19.36), and adenocarcinoma

© AME Publishing Company.

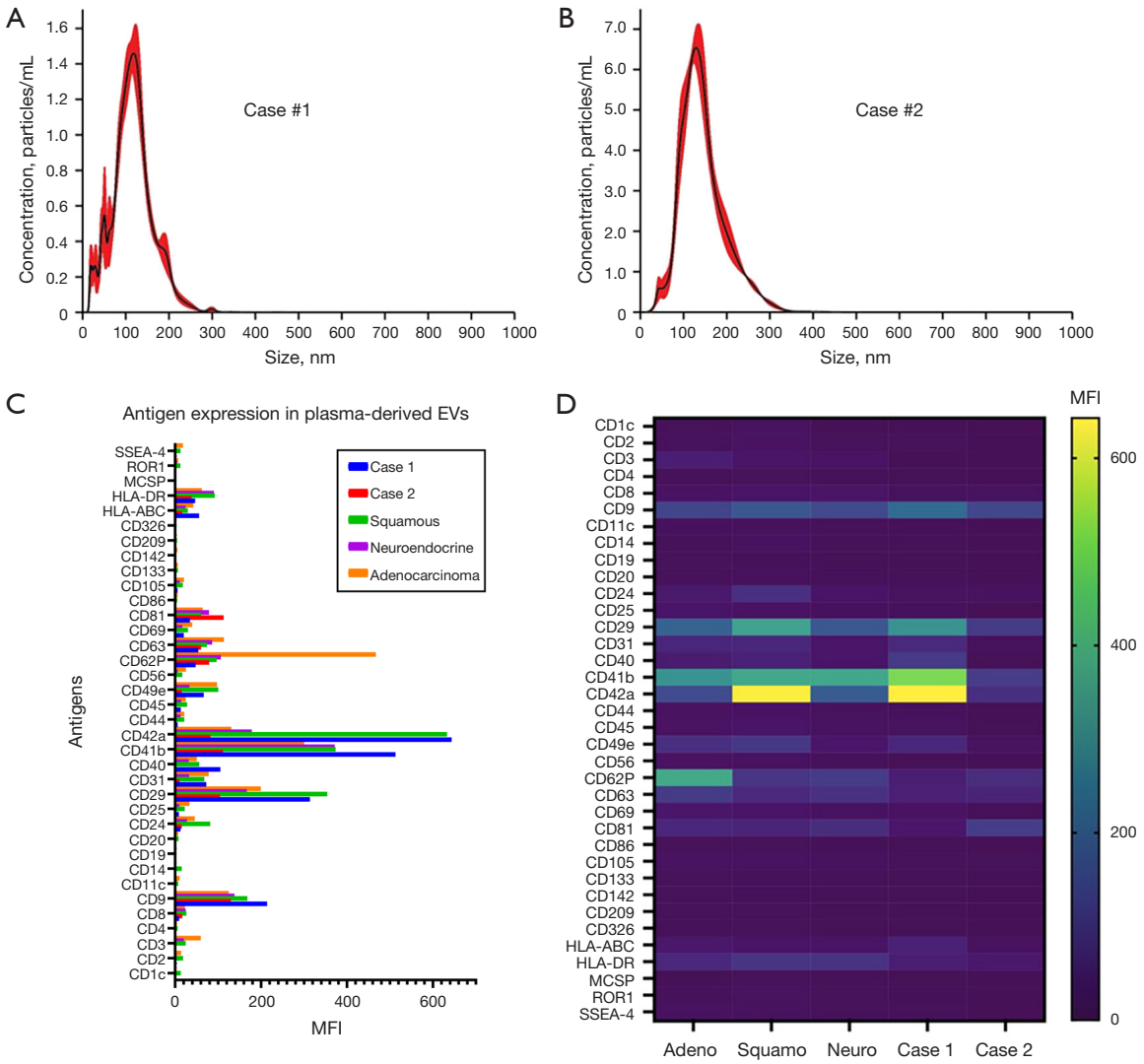

Figure 3 EV analysis. NTA profile analysis of EV-enriched fractions obtained from plasma of (A) case 1 and (B) case 2. Protein expression of each plasma EVs marker by flow cytometry in pleomorphic lung cancer patients reported as (C) bar plot and (D) heatmap. For squamous, neuroendocrine and adenocarcinoma the MFI refers to the median value. The graphs were prepared using GraphPad Prism 8 (Insight Partners, New York City, NY, USA). EV, extracellular vesicle; MFI, median fluorescence intensity; NTA, nanoparticle tracking analysis.

(median MFI =58.86) (*Figure 3C,3D*).

Detection and molecular profiling of CTCs

To characterize the elements released into the bloodstream by PC, we searched for CTCs in peripheral blood of patients case 1 and case 2, which was collected prior to surgery. Following recovery, we conducted molecular profiling to assess their CNA profile at whole-genome scale.

Interestingly, through phenotypic analysis, we also detected heterotypic clusters composed of immune CD45+ cells and CTCs in both patients, case 1 (*Figure 4*) and case 2 (*Figure 5*).

More specifically, in patient case 1, we detected 3 heterotypic clusters (*Figure 4A*), of which one (ID: 7912) was subjected to CNA profiling (*Figure 4B*). A chromosomal loss (1 copy) was found in region 19p12 (comprising the centromere). Copy number gains (>2 copies) were found in chromosomes 1q, 2p, 2q, 3q, 4q, 5q, 9q, 11, 12q, 14q, 15q, 19, 20p, 21q, 22q, X. Regions 2q32.2 and 19p13.42 were found at the highest value of copy number (n=11). To get further insights on the potential functional consequences

© AME Publishing Company.

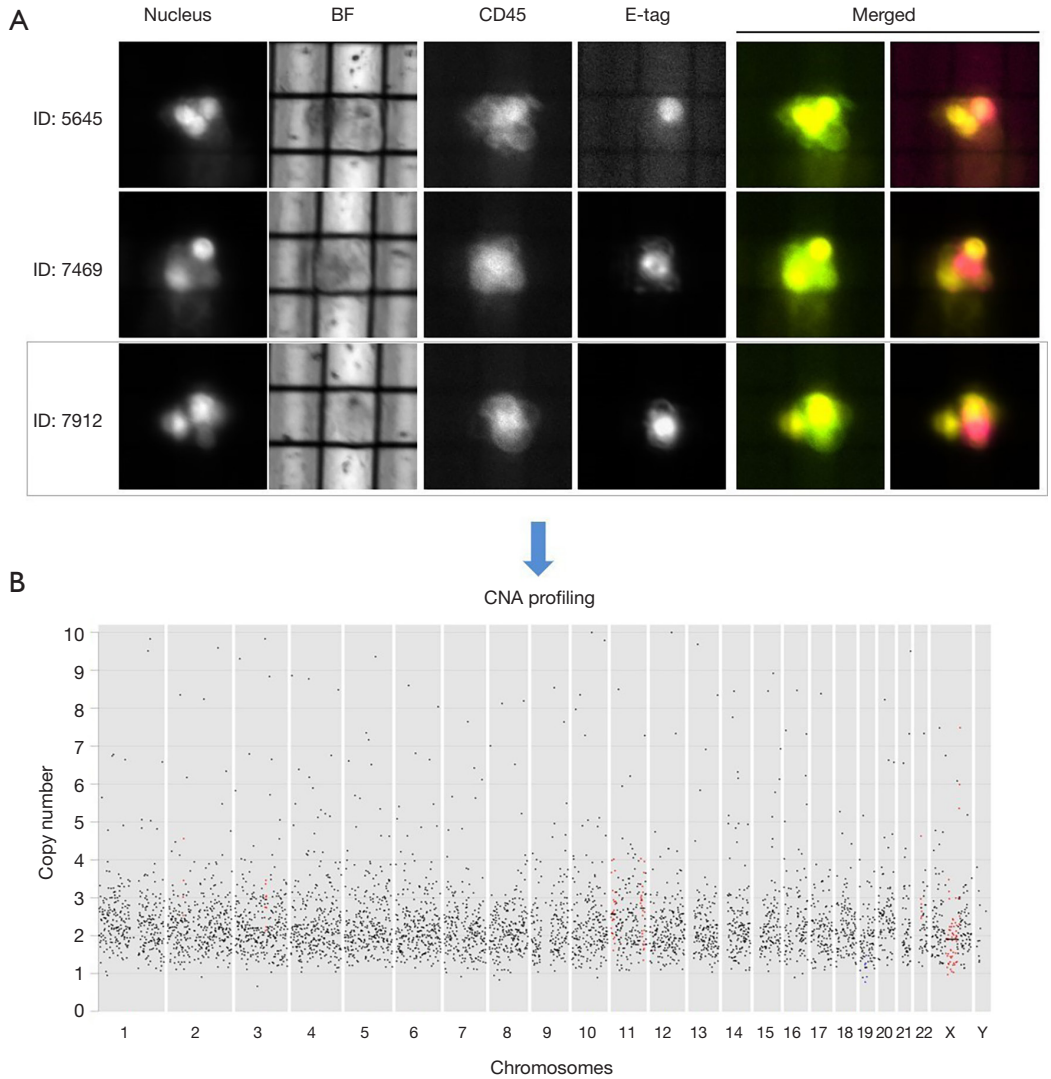

Figure 4 Phenotypic and molecular characterization of detected clusters in case 1. (A) Identification of heterotypic cluster in the bloodstream obtained from case 1 before surgery. (B) The cluster ID: 7912 was subjected to molecular characterization to obtain the whole genome CNA profile. The arrow links the cluster to the matched CNA profile. BF, brightfield; CNA, copy number aberration; ID, identity document.

of detected CNAs, we proceeded with term enrichment. The analysis revealed the enrichment of terms associated with the detection of chemical stimulus involved in sensory perception of smell, phospholipidic efflux and regulation of viral life cycle based on the Gene Ontology Biological Process (GOBP) database.

Concerning patient case 2, we detected and isolated 6 heterotypic clusters. The most representative clusters are reported in *Figure 5A*. All the heterotypic clusters were isolated in a single tube and CNA profiling was performed (*Figure 5B*).

Globally, heterotypic clusters from patient case 2 harboured 7 chromosome losses (chromosomes 3p, 4p, 13q, 16p, 17q, 19p) and 17 chromosome gains (maximum copy number =3 copies; chromosomes 1p, 3q, 8p, 9q, 10q, 12, 13q, 14q, 19q, 20, 21q). To deepen the potential functional consequences of detected CNAs, we performed term enrichment and queried different databases. Through this analysis, we observed the enrichment of pathways associated with mechanistic target of rapamycin (mTOR) regulation, cell cycle, transforming growth factor beta (TGF-β)

© AME Publishing Company.

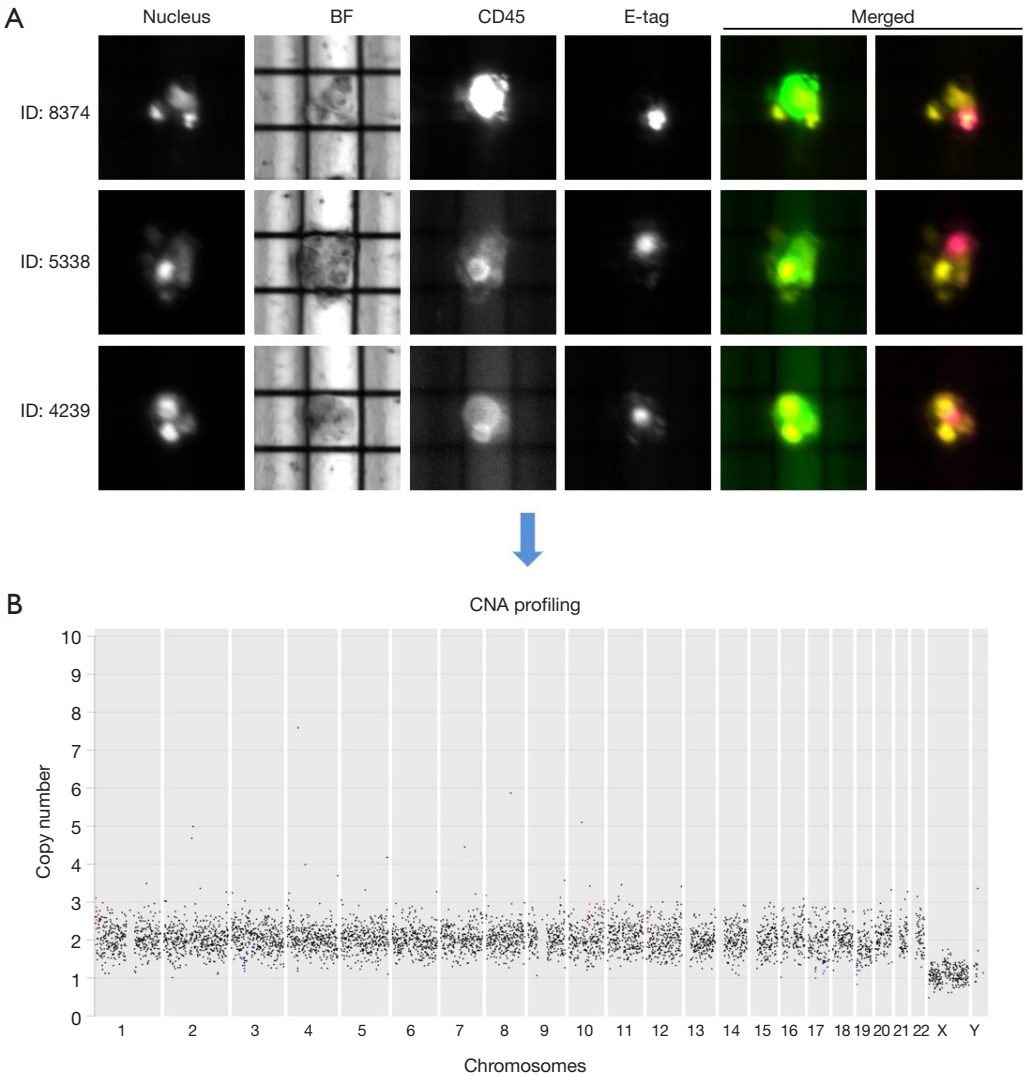

Figure 5 Phenotypic and molecular characterization of detected clusters in case 2. (A) Identification of heterotypic cluster in the bloodstream obtained from case 2 before surgery. (B) All the clusters were isolated in a single tube then subjected to molecular characterization to obtain the whole genome CNA profile. The arrow links the clusters to the matched CNA profile. BF, brightfield; CNA, copy number aberration; ID, identity document.

receptor signaling, and other cancer-associated pathways (*Table 2*).

Discussion

Over the past few years, there has been a greater interest in understanding the molecular background and genomic trajectories of PC and in identifying therapeutic opportunities in this remarkably heterogeneous and aggressive NSCLC subtype (19,20). This is due to the availability of molecular technologies for comprehensive molecular tumor profiling of archived cancer tissue (19,20). In an initial analysis, we characterized the epitopes expressed by plasma-derived EVs from PC patients before surgery using the MACSplex assay (21,22). In patient case 2, we detected a higher concentration of EVs per mL of plasma, consistent with the patient's COPD diagnosis (23). Our results showed that the most prominently expressed epitopes were CD42 and CD41b, both of which are well-known platelet markers. Interestingly, recent

© AME Publishing Company.

Table 2 A list of cancer-associated enriched terms with statistical significance (P<0.05) was generated using genes annotated in aberrant regions identified from CNA profiling of CTCs from patient case 2

Database	Term	Genes	Overlap	P value
GOBP	Regulation of TOR signaling (GO:0032006)	*NPRL3; MLST8; TNFAIP8L1; TSC2; TSC1; ITFG2; WDR24; TELO2*	8/78	0.008
	Negative regulation of TOR signaling (GO:0032007)	*STK11; NPRL3; TNFAIP8L1; TSC2; TSC1; ITFG2; WDR24*	7/54	0.004
KEGG	mTOR signaling pathway	*MAP2K2; NPRL3; TSC2; TSC1; FZD10; WDR24; RHOA; STK11; RPS6KB1; DVL1; MLST8; ULK1; TELO2*	13/154	0.005
Wikipathways	TOR signaling WP1471	*RPS6KB1; MLST8; TSC2; TSC1; ULK1*	5/36	0.01
	Wnt signaling pathway WP363	*DVL1; AXIN1; TSC2; TSC1; TCF3; RHOA*	6/52	0.01
KEGG	PI3K-Akt signaling pathway	*MAP2K2; VWF; LAMB2; TSC2; TSC1; GNG13; FGF6; STK11; RXRA; CCND2; EFNA2; CREB3L3; RPS6KB1; GNG7; NTF3; GNB1; PPP2R2D; MLST8; FGF23; FGF22*	20/354	0.04
	Hippo signaling pathway	*APC2; TEAD4; CCND2; DLG5; DVL1; PPP2R2D; AXIN1; FZD10; AMH; PRKCZ; TP73*	11/163	0.04

CAN, copy number aberration; CTC, circulating tumor cell; GOBP, Gene Ontology Biological Process; KEGG, Kyoto Encyclopedia of Genes and Genomes; mTOR, mechanistic target of rapamycin; TOR, target of rapamycin.

studies have demonstrated that lung cancer cells can hijack platelets by phagocytosing and recycling platelet membrane proteins, such as CD42a, to evade immune surveillance (21). Consistent with these findings, the presence of EVs expressing platelet markers in our study suggests a potential mechanism by which PC tumors might escape immune detection.

Furthermore, when comparing the epitope expression of PC-derived EVs with those from patients with other types of lung cancer, we noted the absence of CD3 expression, a marker for T cells (24). This observation, in line with other results, may reflect a specific involvement of the immune system in the pathophysiology of PC.

Concerning CTCs, recent findings indicate that approximately 30% of patients with early-stage NSCLC (stages I–IIIA, regardless of tumor histology) have detectable preoperative CTCs in their bloodstream, using a cut-off of 5 cells. However, CTC monitoring in this setting is not recommended as a reliable biomarker for minimal residual disease after surgery. Further molecular characterization of CTCs could provide insights into their biology, potentially clarifying their role in a translational context (25). Accordingly, molecular characterization of CTCs may be helpful to better understand the biology of PC. To the best of our knowledge, this is the first report of CTCs in PC.

In both PC cases analyzed in this series, we identified CTCs forming heterotypic clusters with CD45+ cells, as revealed by DEPArray™ phenotypic analysis. A study by Fina *et al.*, involving 74 NSCLC patients across stages I–IV, reported heterotypic clusters in 31.1% of cases. Importantly, the prognostic significance of these clusters was evident only in stage III–IV patients, where their presence was associated with an increased risk of disease recurrence (26). In advanced stages, the detection of these clusters acts as an independent negative prognostic factor (27). Conversely, in early-stage disease, the presence of clusters may reflect interactions between CTCs and components of the liquid microenvironment, potentially influencing disease progression. In a previous report on a patient with metastatic metaplastic breast cancer, we demonstrated that CTC investigation could provide valuable insights into tumor cell morphology, as we observed a high number of both spindle- and round-shaped CTCs (28). In the present study, both PC patients had early-stage disease, resulting in a very low number of detectable CTCs. Furthermore, the presence of clusters further limits the ability to accurately assess CTC morphology.

Molecular profiling of the isolated CTCs in our PC cases revealed several genes located in aberrant regions that play a crucial role in solid tumors, including lung cancer. For example, patient case 1 showed the gain of regions containing the genes *ABL1* (9q34.2), *IGF2* (11p15.5), and *HRAS* (11p15.5), while patient case 3 had loss of regions

© AME Publishing Company.

containing genes of *TSC2* (16p13.3), *RBM5* and *RBM6* (3p21.31), and gain of *CCND2* (12p13.32). The enriched terms identified through this profiling were associated with pathways previously reported in lung cancer literature. Notably, in patient case 2, pathways associated with mTOR were significantly enriched, suggesting a role for this pathway in disease progression and blood-borne dissemination. The mTOR pathway has been extensively studied and is known to play a critical role in lung cancer progression and metastasis, making it a promising target for novel anti-cancer therapies (29). Abnormal activation of this pathway has also been linked to an increased risk of brain metastasis in lung cancer patients, consistent with the clinical history of patient case 2 (30). Although our analysis focused on CTCs from only two PC patients, no common alterations were observed between them. This heterogeneity aligns with the variability seen at the primary tumor level, where the proportions of epithelial and stem cells differed between the two cases. We believe that liquid biopsy through the identification and characterization of blood cells specific for each solid cancer may act as future targets not only in NSCLC, but also in each specific histotypes as for PC of the lung, to better characterize the possible relation between the presence of CTCs, EVs and high grade of malignancy and possible consequent connection to death and/or recurrence.

Since PC is a rare subtype of lung cancer, our analysis is based on a small number of cases, representing the major limitation of our study. This represents a major challenge, as examining samples from only two PC patients limits the statistical power of the study, making it primarily descriptive. However, to the best of our knowledge, this is the first study to describe plasma-derived EVs and CTCs in patients with operable PC, and our findings contribute to a deeper understanding of the disease (31).

Conclusions

This study offers new descriptive insights into PC, a rare and aggressive subtype of NSCLC, by profiling EVs and CTCs from plasma. Findings suggest immune-evasive properties in PC, marked by platelet-related EVs markers and specific CTC features, alongside genetic alterations in pathways like mTOR that are implicated in disease progression. Although limited by a small sample size, this preliminary analysis lays the groundwork for further exploration into PC's unique molecular characteristics, potentially guiding future research on targeted approaches for this challenging cancer subtype. Further studies will need to be set in order to set new perspectives regarding liquid biopsy for this rare tumor.

Acknowledgments

We would like to thank the patients and their families/caregivers for their participation. This work was partly supported by the contribution of Ricerca Corrente from the Italian Ministry of Health.

Footnote

Reporting Checklist: The authors have completed the CARE reporting checklist. Available at https://tlcr.amegroups.com/article/view/10.21037/tlcr-2024-1275/rc

Peer Review File: Available at https://tlcr.amegroups.com/article/view/10.21037/tlcr-2024-1275/prf

Funding: This work was partly supported by the contribution of Ricerca Corrente from the Italian Ministry of Health.

Conflicts of Interest: All authors have completed the ICMJE uniform disclosure form (available at https://tlcr.amegroups.com/article/view/10.21037/tlcr-2024-1275/coif). The authors have no conflicts of interest to declare.

Ethical Statement: The authors are accountable for all aspects of the work in ensuring that questions related to the accuracy or integrity of any part of the work are appropriately investigated and resolved. All procedures performed in this study were in accordance with the Declaration of Helsinki and its subsequent amendments. The present study has been approved by the local ethics committee (Comitato Etico di IRST e di Area Vasta Romagna CEROM, No. IRSTB129). The study complied with the provisions of the Good Clinical Practice guidelines and local laws and fulfilled Regulation (EU) 2016/679 of the European Parliament and the Council of April 27, 2016, on the protection of natural persons regarding the processing of personal data. Written informed consent was obtained from the patient for publication of this case report and accompanying images. A copy of the written consent is available for review by the editorial office of this journal.

Open Access Statement: This is an Open Access article distributed in accordance with the Creative Commons

Attribution-NonCommercial-NoDerivs 4.0 International License (CC BY-NC-ND 4.0), which permits the non-commercial replication and distribution of the article with the strict proviso that no changes or edits are made and the original work is properly cited (including links to both the formal publication through the relevant DOI and the license). See: https://creativecommons.org/licenses/by-nc-nd/4.0/.

References

1. Rodak O, Peris-Díaz MD, Olbromski M, et al. Current Landscape of Non-Small Cell Lung Cancer: Epidemiology, Histological Classification, Targeted Therapies, and Immunotherapy. Cancers (Basel) 2021;13:4705.
2. Rossi G, Russo A, Tagliamento M, et al. Precision Medicine for NSCLC in the Era of Immunotherapy: New Biomarkers to Select the Most Suitable Treatment or the Most Suitable Patient. Cancers (Basel) 2020;12:1125.
3. Li W, Liu JB, Hou LK, et al. Liquid biopsy in lung cancer: significance in diagnostics, prediction, and treatment monitoring. Mol Cancer 2022;21:25.
4. Brown NA, Aisner DL, Oxnard GR. Precision Medicine in Non-Small Cell Lung Cancer: Current Standards in Pathology and Biomarker Interpretation. Am Soc Clin Oncol Educ Book 2018;38:708-15.
5. Lv C, Fang W, Wu N, et al. Osimertinib as neoadjuvant therapy in patients with EGFR-mutant resectable stage II-IIIB lung adenocarcinoma (NEOS): A multicenter, single-arm, open-label phase 2b trial. Lung Cancer 2023;178:151-6.
6. Andrikou K, Rossi T, Verlicchi A, et al. Circulating Tumour Cells: Detection and Application in Advanced Non-Small Cell Lung Cancer. Int J Mol Sci 2023;24:16085.
7. Ma L, Guo H, Zhao Y, et al. Liquid biopsy in cancer current: status, challenges and future prospects. Signal Transduct Target Ther 2024;9:336.
8. Hamilton G, Rath B, Stickler S. Significance of circulating tumor cells in lung cancer: a narrative review. Transl Lung Cancer Res 2023;12:877-94.
9. Passaro A, Al Bakir M, Hamilton EG, et al. Cancer biomarkers: Emerging trends and clinical implications for personalized treatment. Cell 2024;187:1617-35.
10. Mamdani H, Matosevic S, Khalid AB, et al. Immunotherapy in Lung Cancer: Current Landscape and Future Directions. Front Immunol 2022;13:823618.
11. Ma Y, Zhang X, Liu C, et al. Extracellular vesicles in cancers: mechanisms, biomarkers, and therapeutic strategies. MedComm (2020) 2024;5:e70009.
12. Makler A, Asghar W. Exosomal biomarkers for cancer diagnosis and patient monitoring. Expert Rev Mol Diagn 2020;20:387-400.
13. Ouziane I, Boutayeb S, Mrabti H, et al. Sarcomatoid carcinoma of the lung: a model of resistance of chemotherapy. N Am J Med Sci 2014;6:342-5.
14. Li X, Wu D, Liu H, et al. Pulmonary sarcomatoid carcinoma: progress, treatment and expectations. Ther Adv Med Oncol 2020;12:1758835920950207.
15. Ferrarini A, Forcato C, Buson G, et al. A streamlined workflow for single-cells genome-wide copy-number profiling by low-pass sequencing of LM-PCR whole-genome amplification products. PLoS One 2018;13:e0193689.
16. Gallerani G, Rossi T, Valgiusti M, et al. CNA Profiling of Single CTCs in Locally Advanced Esophageal Cancer Patients during Therapy Highlights Unexplored Molecular Pathways. Cancers (Basel) 2021;13:6369.
17. Rossi T, Angeli D, Tebaldi M, et al. Dissecting Molecular Heterogeneity of Circulating Tumor Cells (CTCs) from Metastatic Breast Cancer Patients through Copy Number Aberration (CNA) and Single Nucleotide Variant (SNV) Single Cell Analysis. Cancers (Basel) 2022;14:3925.
18. Masciale V, Grisendi G, Banchelli F, et al. CD44+/EPCAM+ cells detect a subpopulation of ALDH(high) cells in human non-small cell lung cancer: A chance for targeting cancer stem cells? Oncotarget 2020;11:1545-55.
19. Sen T, Takahashi N, Chakraborty S, et al. Emerging advances in defining the molecular and therapeutic landscape of small-cell lung cancer. Nat Rev Clin Oncol 2024;21:610-27.
20. Frank MS, Bodtger U, Gehl J, et al. Actionable Molecular Alterations Are Revealed in Majority of Advanced Non-Small Cell Lung Cancer Patients by Genomic Tumor Profiling at Progression after First Line Treatment. Cancers (Basel) 2021;14:132.
21. Martins Castanheira N, Spanhofer AK, Wiener S, et al. Uptake of platelets by cancer cells and recycling of the platelet protein CD42a. J Thromb Haemost 2022;20:170-81.
22. Wiklander OPB, Bostancioglu RB, Welsh JA, et al. Systematic Methodological Evaluation of a Multiplex Bead-Based Flow Cytometry Assay for Detection of Extracellular Vesicle Surface Signatures. Front Immunol 2018;9:1326.
23. Petraroia I, Ghidotti P, Bertolini G, et al. Extracellular vesicles from subjects with COPD modulate cancer

initiating cells phenotype through HIF-1α shuttling. Cell Death Dis 2023;14:681.
24. Ren Y, Ge K, Tang Q, et al. Dual-Recognition-Mediated Autocatalytic Amplification Assay for the Subpopulations of PD-L1 Positive Extracellular Vesicle. Anal Chem 2024;96:9585-92.
25. Garitaonaindia Y, Aguado-Noya R, Garcia-Grande A, et al. Monitoring with circulating tumor cells in the perioperative setting of patients with surgically treated stages I-IIIA NSCLC. Transl Lung Cancer Res 2023;12:1414-24.
26. Fina E, Federico D, Novellis P, et al. Subpopulations of Circulating Cells with Morphological Features of Malignancy Are Preoperatively Detected and Have Differential Prognostic Significance in Non-Small Cell Lung Cancer. Cancers (Basel) 2021;13:4488.
27. Li Z, Fan L, Wu Y, et al. Analysis of the prognostic role and biological characteristics of circulating tumor cell-associated white blood cell clusters in non-small cell lung cancer. J Thorac Dis 2022;14:1544-55.
28. Rossi T, Palleschi M, Angeli D, et al. Case Report: Analysis of Circulating Tumor Cells in a Triple Negative Spindle-Cell Metaplastic Breast Cancer Patient. Front Med (Lausanne) 2021;8:689895.
29. Tan AC. Targeting the PI3K/Akt/mTOR pathway in non-small cell lung cancer (NSCLC). Thorac Cancer 2020;11:511-8.
30. Li Q, Yang J, Yu Q, Wu H, Liu B, Xiong H, Hu G, Zhao J, Yuan X, Liao Z. Associations between single-nucleotide polymorphisms in the PI3K-PTEN-AKT-mTOR pathway and increased risk of brain metastasis in patients with non-small cell lung cancer. Clin Cancer Res 2013;19:6252-60.
31. Słomka A, Wang B, Mocan T, et al. Extracellular Vesicles and Circulating Tumour Cells - complementary liquid biopsies or standalone concepts? Theranostics 2022;12:5836-55.

Cite this article as: Rossi T, Cortesi M, Zanoni M, Bandini S, Sbrighi C, Angeli D, Masciale V, Grisendi G, Costantini M, Stella F, Ulivi P, Aramini B. Liquid biopsy perspectives in pleomorphic carcinoma of the lung: case report. Transl Lung Cancer Res 2025;14(6):2324-2336. doi: 10.21037/tlcr-2024-1275

© AME Publishing Company.